Research Article | Vol. 25, No. 19 | 18 Sep 2017 | OPTICS EXPRESS 22499
Optics EXPRESS

Active intensity noise suppression for a broadband mid-infrared laser source

MARINUS HUBER,[1,2,*] WOLFGANG SCHWEINBERGER,[1,3] FABIAN STUTZKI,[4] JENS LIMPERT,[4] IOACHIM PUPEZA,[1,2] AND OLEG PRONIN[2]

[1]*Ludwig-Maximilians-Universität München, Am Coulombwall 1, 85748 Garching, Germany*
[2]*Max-Planck-Institut für Quantenoptik, Hans-Kopfermann-Straße 1,85748 Garching, Germany*
[3]*King Saud University, Department of Physics and Astronomy, Riyadh 11451, Saudi Arabia*
[4]*Friedrich-Schiller-University Jena, Institute of Applied Physics, Albert-Einstein-Straße 15, 07745 Jena, Germany*
*marinus.huber@mpq.mpg.de

Abstract: Excess relative intensity noise (RIN) constitutes one of the major limitations of most spectroscopic methods involving lasers. Here, we present an active RIN suppression scheme for a coherent mid-infrared (MIR) light source (8.4-11 µm), based on intra-pulse difference frequency generation (DFG). Three different stabilization concepts that rely on modulating the intensity of the driving near-infrared (NIR) pulse train with an acousto-optic modulator are investigated and compared. By using the wings of the NIR spectrum to generate the error signal, a RIN suppression of the MIR pulse train of up to a factor of 20 was achieved in the band between 1 Hz and 100 kHz, resulting in a total integrated RIN of 0.07%.

OCIS codes: (140.3425) Laser stabilization; (140.3070) Infrared and far-infrared lasers.

References and links

1. P. C. Hobbs, "Ultrasensitive laser measurements without tears," Appl. Opt. **36**(4), 903–920 (1997).
2. J. Hodgkinson and R. P. Tatam, "Optical gas sensing: a review," Meas. Sci. Technol. **24**(1), 012004 (2013).
3. P. Kwee, C. Bogan, K. Danzmann, M. Frede, H. Kim, P. King, J. Pöld, O. Puncken, R. L. Savage, F. Seifert, P. Wessels, L. Winkelmann, and B. Willke, "Stabilized high-power laser system for the gravitational wave detector advanced LIGO," Opt. Express **20**(10), 10617–10634 (2012).
4. F. Seifert, P. Kwee, M. Heurs, B. Willke, and K. Danzmann, "Laser power stabilization for second-generation gravitational wave detectors," Opt. Lett. **31**(13), 2000–2002 (2006).
5. O. Pronin, M. Seidel, F. Lücking, J. Brons, E. Fedulova, M. Trubetskov, V. Pervak, A. Apolonski, T. Udem, and F. Krausz, "High-power multi-megahertz source of waveform-stabilized few-cycle light," Nat. Commun. **6**, 6988 (2015).
6. C. Jauregui, J. Limpert, and A. Tünnermann, "High-power fibre lasers," Nat. Photonics **7**(11), 861–867 (2013).
7. S. Hädrich, M. Krebs, A. Hoffmann, A. Klenke, J. Rothhardt, J. Limpert, and A. Tünnermann, "Exploring new avenues in high repetition rate table-top coherent extreme ultraviolet sources," Light Sci. Appl. **4**(8), e320 (2015).
8. I. Pupeza, D. Sánchez, J. Zhang, N. Lilienfein, M. Seidel, N. Karpowicz, I. Znakovskaya, M. Pescher, W. Schweinberger, V. Pervak, E. Fill, O. Pronin, Z. Wei, F. Krausz, A. Apolonski, and J. Biegert, "High-power sub-two-cycle mid-infrared pulses at 100 MHz repetition rate," Nat. Photonics **9**(11), 721 (2015).
9. C. Kötting and K. Gerwert, "Monitoring protein–ligand interactions by time-resolved FTIR difference spectroscopy," Protein-Ligand Interact. Methods Appl. **1008**, 299–323 (2013).
10. P. Lerch, P. Dumas, T. Schilcher, A. Nadji, A. Luedeke, N. Hubert, L. Cassinari, M. Boege, J. C. Denard, L. Stingelin, L. Nadolski, T. Garvey, S. Albert, Ch. Gough, M. Quack, J. Wambach, M. Dehler, and J. M. Filhol, "Assessing noise sources at synchrotron infrared ports," J. Synchrotron Radiat. **19**(Pt 1), 1–9 (2012).
11. S. Keiber, S. Sederberg, A. Schwarz, M. Trubetskov, V. Pervak, F. Krausz, and N. Karpowicz, "Electro-optic sampling of near-infrared waveforms," Nat. Photonics **10**(3), 159–162 (2016).
12. J. Zhang, J. Brons, N. Lilienfein, E. Fedulova, V. Pervak, D. Bauer, D. Sutter, Z. Wei, A. Apolonski, O. Pronin, and F. Krausz, "260-Megahertz, Megawatt-Level Thin-Disk Oscillator," Opt. Lett. **40**(8), 1627–1630 (2015).
13. P. Kwee, B. Willke, and K. Danzmann, "Shot-noise-limited laser power stabilization with a high-power photodiode array," Opt. Lett. **34**(19), 2912–2914 (2009).
14. N. R. Newbury, B. R. Washburn, K. L. Corwin, and R. S. Windeler, "Noise amplification during supercontinuum generation in microstructure fiber," Opt. Lett. **28**(11), 944–946 (2003).
15. U. Møller, S. T. Sørensen, C. Jakobsen, J. Johansen, P. M. Moselund, C. L. Thomsen, and O. Bang, "Power dependence of supercontinuum noise in uniform and tapered PCFs," Opt. Express **20**(3), 2851–2857 (2012).

#297992 https://doi.org/10.1364/OE.25.022498
Journal © 2017 Received 15 Jun 2017; revised 16 Aug 2017; accepted 16 Aug 2017; published 7 Sep 2017

Optics EXPRESS

16. A. Leitenstorfer, S. Hunsche, J. Shah, M. C. Nuss, and W. H. Knox, "Detectors and sources for ultrabroadband electro-optic sampling: Experiment and theory," Appl. Phys. Lett. **74**(11), 1516–1518 (1999).
17. A. A. Lanin, A. A. Voronin, A. B. Fedotov, and A. M. Zheltikov, "Time-domain spectroscopy in the mid-infrared," Sci. Rep. **4**(1), 6670 (2015).

1. Introduction

The intensity noise of the laser source represents a significant limitation on any high-precision optical measurement. While some spectroscopic measurements, such as those that employ balanced detection, rely on passive intensity noise suppression [1,2] or mitigate the influence of excess relative intensity noise (RIN) by using modulation techniques (several of which are reviewed in Ref [2].), other applications require active stabilization of the laser source itself. For instance, in gravitational wave detectors a complex active stabilization scheme is implemented which allows to suppress radiation pressure fluctuations on the mirrors that originate from laser intensity noise [3,4]. A stable laser source is also vital for driving nonlinear (optical) processes [1]. The radiation emitted by these sources (usually in the visible or near-infrared [5,6]) can be converted via nonlinear processes to achieve broad spectral coverage ranging from the extreme ultraviolet [7] to the mid- and far infrared [8]. The unique combination of high brightness with unparalleled spatial and temporal coherence makes mode-locked, MHz-repetition-rate lasers indispensable for high-precision metrology in these spectral regions.

Particularly in the mid-infrared (MIR) region, such sources are of great interest for vibrational spectroscopy. This technique allows organic compounds in gases or liquids to be identified in a label-free manner by their unique molecular fingerprints, and finds a large variety of applications in biology, chemistry, medicine and environmental monitoring. Fourier transform infrared (FTIR) spectrometers based on thermal sources ("globar") remain the instrument of choice in the field [9]. However, even though thermal sources only exhibit low intensity noise, the performance of these devices is usually limited by detector noise rather than by photon shot noise, owing to the weak light intensity of thermal sources.

Laser-based MIR sources could in principle overcome this problem thanks to their high brightness; however, one of the major limitations of these sources is their (low-frequency) RIN, which usually lies orders of magnitude above the power-equivalent shot-noise limit. In order to reduce this excess noise contribution, most MIR spectroscopic techniques (like FTIR spectroscopy) employ fast scanning (or other modulation techniques) to effectively transfer the measured spectrum into a radio frequency region with lower noise levels. With mechanical delay stages, scan speeds of 10 mm/s can easily be obtained, shifting the noise contribution for spectral components at 1000 cm^{-1} to noise frequencies around 2 kHz [10]. However, with laser sources, noise in the kHz frequency range is normally dominated by strong excess noise, and therefore further reduction of RIN is highly desirable.

In this work, we present an active intensity noise suppression system for a coherent source of broadband MIR radiation generated by a 19-fs near-infrared (NIR) pulse train via intra-pulse difference-frequency-generation (DFG), which is based on an acousto-optic-modulator (AOM). Three different stabilization concepts are investigated and compared. As direct stabilization of the generated MIR can be very challenging owing to the lack of sufficiently sensitive broadband detectors and/or active broadband optical elements in the MIR spectral range, all investigated stabilization concepts aim at stabilizing the driving source itself. In addition, the error signal for the feedback loop is generated with a pick-off from the driving NIR source. This circumvents the need for rather impractical and less sensitive liquid-nitrogen-cooled mercury cadmium telluride (MCT) photodetectors for the MIR radiation. Combined with MIR detection schemes that rely on frequency up-conversion, such as EOS [8,11], this could lead to highly sensitive MIR spectroscopy without the requirement to use MIR detectors which require liquid nitrogen cooling.

We demonstrate that the implementation of this stabilization system results in the suppression of RIN of the generated MIR by up to a factor of 20 (in the band between 1 Hz

Optics EXPRESS

and 20 kHz). The concept presented here can significantly broaden the application of laser-based mid-infrared sources in spectroscopy.

2. Experimental setup

The experimental setup is shown in Fig. 1(a). The output of an Yb:YAG Kerr-lens mode-locked thin-disc oscillator [12] (100 MHz, 260 fs, up to 70 W) is spectrally broadened in a photonic crystal fiber (PCF) and temporally compressed by chirped mirrors [5]. The resulting 19-fs pulses (measured with frequency-resolved optical gating) are focused into a 1-mm thick $LiGaS_2$ (LGS) crystal to create, via intra-pulse difference frequency generation (DFG), broadband ultrashort MIR pules with a central wavelength of 10 µm and an average power of 5 mW [8]. The pulse duration of 65 fs was determined via electro-optical sampling [8] and the MIR spectrum was measured with a FITR spectrometer (Lasnix, L-FTS). To achieve optimum intensity stability, the nonlinear broadening in the PCF and the DFG process are driven at lower average powers here than in Ref [8].

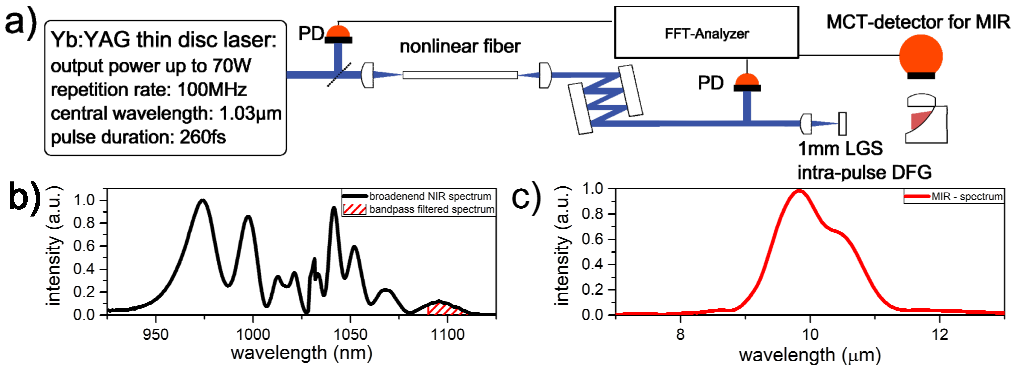

Fig. 1. a) Schematic of the free-running laser setup. The NIR pulses from the oscillator are spectrally broadened in a nonlinear fiber and temporally compressed by chirped mirrors (CM). The resulting 19-fs pulse train is focused into a LiGaS2 crystal to generate MIR radiation via intra-pulse difference frequency generation. Fluctuations in the power of the free-running NIR or MIR radiation were measured with photodiodes (PD) at different positions in the setup, and the noise spectrum was recorded with a fast Fourier transform analyzer. b) Optical spectrum of the broadened NIR light. The patterned area indicates the portion of the spectrum that was used for generation of the feedback signal in stabilization concepts Ib and IIIb. c) Optical MIR spectrum measured with a FTIR.

The strategies for intensity stabilization of the MIR pulses described here rely on the use of an AOM as an active optical element to control the transmitted power. In the free-running state, 98% of the intensity is transmitted through the AOM (the 0th-order beam), while 2% is diffracted to higher orders and discarded. The error signal for the DC-coupled feedback loop is generated by diverting a fraction of the main NIR beam and detecting it with a 2-mm diameter InGaAs amplified photodiode (Thorlabs, PDA20CS).

The signal generated with the in-loop photodiode is then fed into a PI^2D controller (Vescent Photonics, D2-125) which regulates the RF power of the AOM driver (Intraaction, ME-1104) and therefore provides active feedback on the transmitted laser intensity. The internal voltage reference of the D2-125 is used to define the lock point. The two integrators in the PI^2D loop are set to 200 kHz and 2 MHz, respectively. The differential value and the gain (up to a maximum value of 32 dB) of the loop are then adjusted to attain the best possible noise suppression.

We implemented and compared three concepts for intensity stabilization of the MIR pulses, which differ in the placement of the AOM and the in-loop photodiode within the optical setup (see Fig. 2):

Optics EXPRESS

Concept I: The AOM is placed after the fiber, where generation of the error signal occurs, either without any spectral filtering (Concept Ia) or after passage through a 1100 nm (± 10 nm) bandpass filter (Concept Ib) - Fig. 2(a)

Concept II: The AOM is placed ahead of the fiber and generation of the error signal also occurs in front of the fiber - Fig. 2(b)

Concept III: The AOM is placed ahead of the fiber, while generation of the error signal takes place downstream of the fiber, either without any spectral filtering (Concept IIIa) or after passage through a 1100 nm (± 10 nm) bandpass filter (Concept IIIb) - Fig. 2(c)

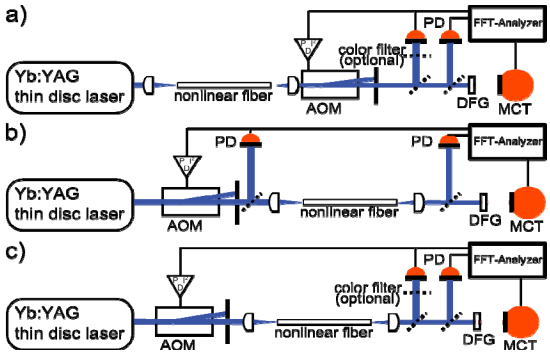

Fig. 2. Schematic of the three stabilization concepts: a) Concept I, b) Concept II, c) Concept III.

For concepts I and III, a fraction of the main beam was diverted via two subsequent 92/8 beam splitters, and an 1100-nm bandpass filter (Thorlabs, FB1100-10) was optionally placed before the photodiode to select only a part of the broadened spectrum for generation of the feedback signal (see Fig. 1(b)). In concept II, the error signal was generated based on the portion of the main beam transmitted through one of the highly reflective dielectric mirrors.

In all cases, additional neutral-density filters were employed to attenuate the laser beam used for generation of the feedback signal to an average power of about 1 mW. The spot size on the detector area (500 µm) was carefully aligned with the center of the diodes to minimize cross-coupling due to beam-pointing fluctuations [4,13]. Note that, in principle, one could also generate the error signal for the stabilization of the MIR intensity by directly measuring the MIR fluctuations with a mercury cadmium telluride (MCT) detector. However, this would require liquid nitrogen cooling, reduce the versatility of the approach and compromise long-term usage.

The independent (out-of-loop) MIR signal was recorded by focusing the beam onto a liquid-nitrogen-cooled MCT detector (Kolmar Technologies, KMPV11-0.25-J1/DC50). The voltage noise spectrum (in $[V/Hz^{0.5}]$ up to 100 kHz) was recorded with a fast Fourier transform (FFT) spectrum analyzer (Stanford Research, SR780) and normalized by the DC voltage signal to obtain the relative intensity noise spectrum s_{RIN} [in $1/Hz^{0.5}$]. The integrated root-mean-square (rms) RIN value for a given bandwidth was obtained by:

$$RIN_{rms}(f_0, f_1) = \sqrt{\int_{f_0}^{f_1} \left(s_{RIN}(f)\right)^2 df} \qquad (1)$$

The NIR out-of-loop signal was recorded using the same photodiode and pick-off optics as for generation of the in-loop signal. The noise suppression results for the NIR beam are discussed in more detail in the Appendix. The whole setup was encased in a housing to

Optics EXPRESS

minimize air fluctuations. Additionally, all photodiodes were placed in an additional housing to minimize the influence of scattered light on the noise suppression.

3. Results

First, the RIN spectra of the oscillator, the nonlinearly broadened NIR pulse train, the red edge of the broadened NIR pulses (at 1100 nm ± 10 nm) and the MIR radiation were measured without active stabilization (see Fig. 3). The integrated RIN (rms, from 1Hz to 100 kHz) of the oscillator (black curve) is 0.1% and the noise spectrum shows the typical *1/f* behavior. Nonlinear broadening does not change the RIN when the entire optical spectrum of the broadened NIR pulses is considered (blue curve, Fig. 3). However, the RIN of the edge of the broadened spectrum (at 1100 nm ± 10 nm, violet curve, Fig. 3) is increased by a factor of ~11 over the measured RF spectrum. Approximately the same increase in noise was observed when the RIN of the blue edge of the NIR spectrum was measured (with a 950-nm shortpass filter, data not shown). The fact that the noise within one region of the broadened spectrum is amplified relative to the total input fluctuations is well-known, and has been reported and investigated by several groups [14,15]. In contrast, the fluctuations of the entire broadened NIR spectrum (i.e. integrated over all wavelengths) are approximately proportional to the input fluctuations (if no losses occur, the output power of the fiber is equal to the input power). The overall MIR noise spectrum (red, Fig. 3) is very similar to the noise at the edge of the spectrum. This can be attributed to the fact that, in this DFG scheme, the outer portions of the NIR spectrum are mixed.

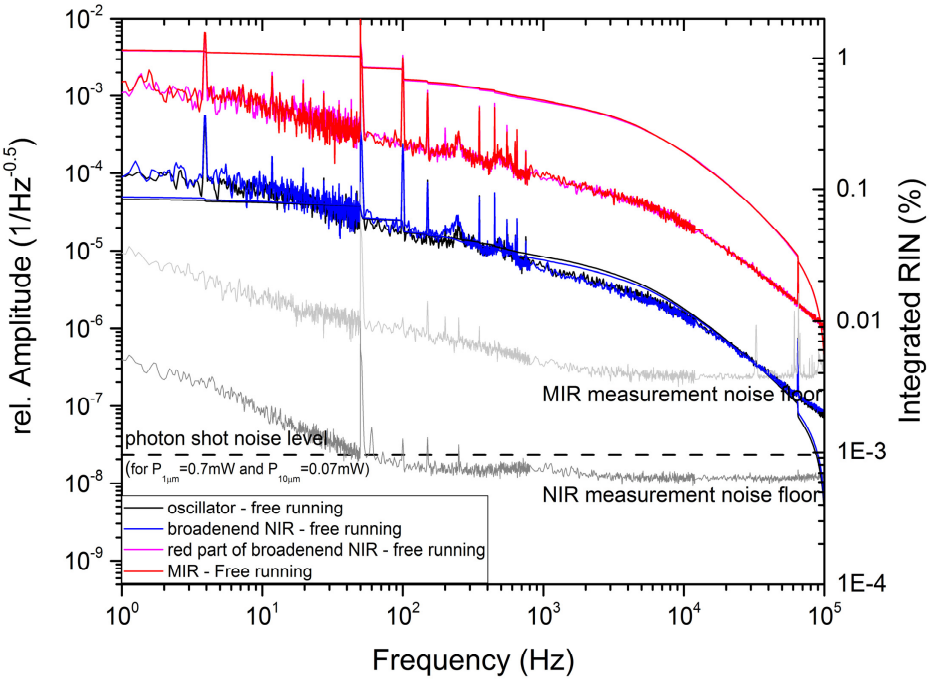

Fig. 3. Relative intensity noise and integrated noise (integration starts at 100 kHz) of the free-running system for the oscillator (black), the broadened NIR (blue), the red portion of the broadened NIR spectrum (pink) and the MIR light (red). The measurement noise floors of the InGaAs and MCT detectors are both well below the relative intensity noise of the measured radiation.

The extents of noise suppression of the MIR achieved by the three aforementioned stabilization concepts are shown in Figs. 4 and 5, respectively.

Optics EXPRESS

Implementation of stabilization concept I (AOM in front of the fiber and generation of the error signal in front of the fiber) reduces the MIR noise by up to a factor of 3 for frequencies below 50 kHz, while the integrated noise (rms, 1 to 100 kHz) was reduced from 1.2% to 0.5% (see Fig. 4(b)).

In concept II, the error signal generated downstream of the fiber was fed back to an AOM placed after the fiber. This signal was either obtained from the full optical NIR spectrum or produced after passage through an additional bandpass filter at 1100 nm, but no suppression of the MIR noise was observed in either of these cases (see Fig. 4(a)). In contrast, use of the same configuration to derive the error signal for NIR results in strong suppression of the RIN (see Appendix, Fig. 6(b)).

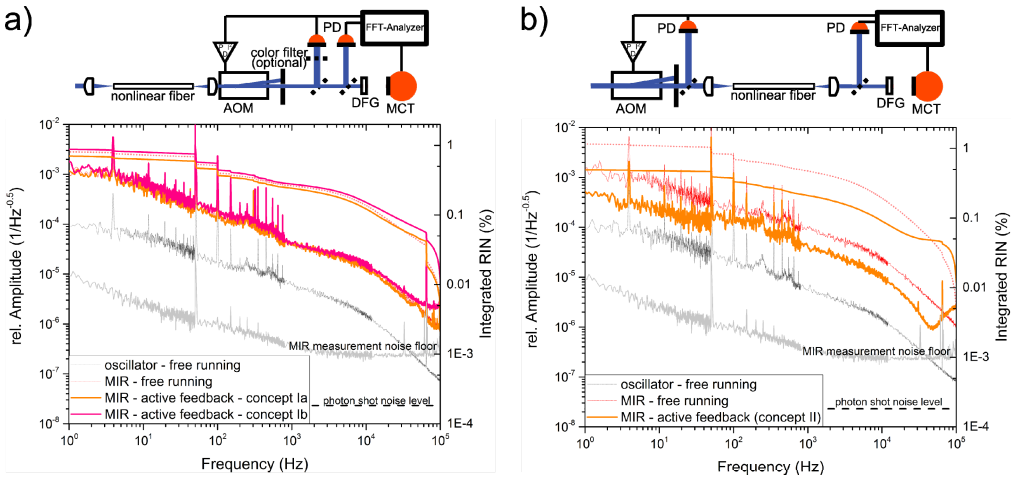

Fig. 4. MIR noise suppression by stabilization concepts I and II. No MIR noise reduction was achieved with stabilization concept I (a) while moderate suppression (by a factor of ~3) was obtained with stabilization concept II (b). A sketch of the stabilization concept employed is shown above each graph.

For stabilization concept III an error signal derived after the nonlinear broadening was fed back to the AOM in front of the fiber. As in concept I, the error signal was either generated from the full spectrum or from the red edge of the broadened spectrum. Application of the first approach suppressed the intensity noise by up to a factor of 5, whereas the second option led to noise reduction by up to a factor of 20 relative to the RIN of the free-running MIR for frequencies below 20 kHz. The corresponding integrated noise level (rms, 1 Hz to 100 kHz) was 0.3% or 0.07%, respectively (see Fig. 5(a)). Similar noise suppression is achieved when the blue edge of the spectrum is used to generate the error signal (data not shown).

In summary, stabilization concept IIIb (AOM placed in front of the fiber and generation of the error signal placed after the fiber with the edge of the optical spectrum) achieves the strongest suppression of MIR noise. Using this setup, the long-term stability of the MIR was tested. Figure 5(c)) shows a normalized time trace of the MCT signal recorded, with and without active feedback, by an FFT analyzer over a period of 500s (this measurement is equal to a frequency noise bandwidth of 2 mHz to 2 Hz). The measured power fluctuations during this period are below 0.05% rms. Stabilization on longer time scales is limited by thermal drifts within the system.

Optics EXPRESS

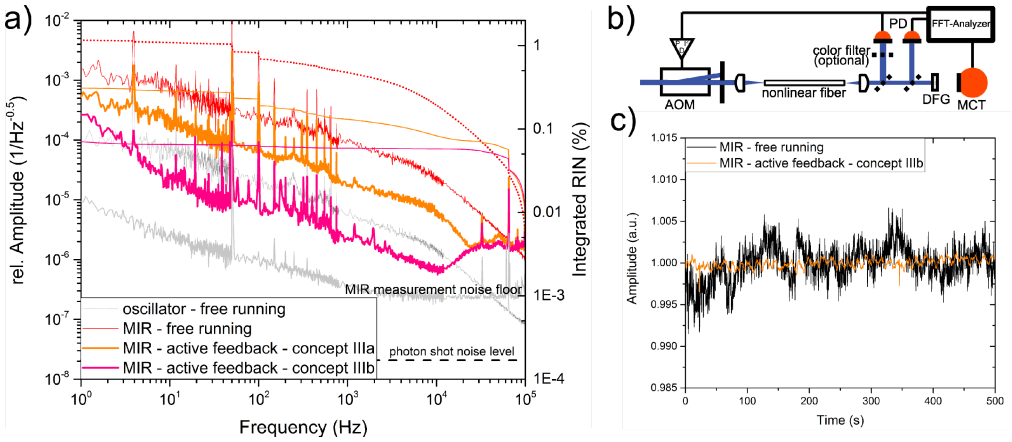

Fig. 5. a) MIR noise suppression by stabilization concept III. b) Sketch of the experimental layout for stabilization concept III. c) Normalized intensity fluctuations of the stabilized (concept IIIb) MIR beam (orange) recorded over 500s with an FFT analyzer. The rms of the intensity fluctuations of the stabilized beam is less than 0.05%.

4. Discussion

The three stabilization concepts investigated here yielded very different degrees of MIR noise suppression. While concepts II and III resulted in noise reduction by factors of up to 10 and 20, respectively, no suppression of MIR noise was observed for stabilization concept I.

This outcome can be explained by variations in the magnitude of nonlinear broadening in the photonic crystal fiber, which results in corresponding differences in the amplification of noise in the broadened spectrum [14]. Moreover, the noise levels in the blue and red edges of the spectrum may be uncorrelated to some extent. An increase in input energy into the nonlinear fiber due to intensity fluctuations may thus lead to a higher power spectral density (PSD) in one part of the spectrum and to a lower PSD in another. If the AOM is placed downstream of the broadening fiber, the stabilization can act either on the noise contained in the entire optical spectrum or only on the fraction associated with the selected part of it (e.g. the red edge). Hence, this stabilization scheme does not permit one to simultaneously stabilize separate regions of the optical spectrum, which might fluctuate independently. However, simultaneous stabilization of different parts of the optical spectrum is precisely what is required to stabilize the output of an intra-pulse DFG scheme, as it is the mixing of the blue and red edges of the spectrum that leads to MIR generation.

Stabilization concept II suppresses the noise of the NIR pulse train before it enters the nonlinear fiber. Clearly, a reduction in RIN at the input of the fiber results in a reduction of noise in the broadened spectrum, and therefore suppresses MIR noise. However, as the error signal is generated upstream of the fiber, this scheme cannot compensate for nonlinear noise amplification within the fiber.

In stabilization concept III, on the other hand, the error signal is generated downstream of the fiber and fed back to the AOM, which acts prior to the fiber. First, we tried to stabilize the system using an error signal based on the full broadened optical spectrum. The RIN of the fiber output is very close to the RIN of the input beam, as can be seen in Fig. 3 (black vs. blue). Therefore, the MIR noise reduction is similar to that provided by concept II, in which the error signal was generated in front of the fiber. When only the edge of the broadened spectrum is used, the nonlinear error signal obtained is very sensitive to power fluctuations at the input of the fiber, and is also affected by nonlinear noise amplification during spectral broadening within the fiber. Stabilization of this signal leads to a reduction in the total noise, but also to a reduction in the nonlinear noise amplification during the spectral broadening. This in turn results in an overall noise reduction, which is associated with stronger

Optics EXPRESS

correlations between the intensity fluctuations in the different parts of the optical spectrum. As a result, the strongest suppression of the generated MIR intensity fluctuations – down to a RIN of ≈6 * 10^{-7} k$Hz^{-0.5}$ at 10 kHz – is achieved.

This is still a factor of 20 worse than the shot noise limit attainable for the feedback system, and this discrepancy is exacerbated at lower frequencies. The reason for this is that only the intensity fluctuations common to the measured error signal and the actual MIR signal can be canceled out [1]. Any uncorrelated noise signal which exclusively couples into either the in-loop or the out-of-loop signal will degrade the noise suppression performance. The system used here is most likely prone to such uncorrelated noise sources, as two nonlinearities (nonlinear broadening and DFG) are utilized to create the MIR radiation, while the active optical element and the photodiode for the generation of the error signal are working within the NIR wavelength region. Furthermore, due to the broadband nature of the NIR and MIR light, uncorrelated noise in different parts of the optical spectrum will degrade the overall efficiency of noise suppression.

Some additional noise sources were also identified and minimized. Any spatial dependence of the laser noise in combination with beam-pointing fluctuations can couple to the measured laser intensity due to the non-uniform response of the photodiodes [4]. As the beam pointing and the spatial response will differ for each photodiode, this will lead to uncorrelated noise that cannot be further suppressed. This noise source becomes dominant at low frequencies, due to the typical timescale of air fluctuations. In order to minimize this cross-coupling, the complete laser setup was enclosed in a housing to reduce the air fluctuations. In its absence of this precaution, the out-of-loop noise suppression was significantly degraded. Encasing the setup in a pressure-tight housing with clean air or in a vacuum enclosure might improve the noise suppression performance further.

The noise spectrum shows spikes at multiple values of 50 Hz, which indicates coupling of the power supply into the feedback loop or photodiode signals. In principle, these noise contributions can be suppressed by driving the electronics with batteries or stable DC sources. There is also a strong noise contribution at 4 Hz, which can probably be attributed to the water cooling of the laser system. Further potential noise sources include uncorrelated temperature fluctuations of both photodiodes, low-frequency noise and bias voltage fluctuations in the photodiodes, mechanical vibrations of the optics, electronic grounding noise, or polarization fluctuations [1,4,13].

As shown in Fig. 5, stabilization concept IIIb also helps to improve the long-term power stability of the MIR light generated. However, this works only over moderate time scales (10 min) before drifts in the average MIR power set in. Such drifts cannot be stabilized solely with the error signal derived from the NIR, as other effects that are independent of the NIR power also contribute. Even if the power of the NIR beam is perfectly stable, the MIR power generated might still vary slightly, as beam pointing drifts will alter the targeted position on the DFG crystal or temperature-dependent MIR generation conditions.

5. Conclusion

We have investigated and compared three different approaches to active intensity stabilization of a broadband MIR source driven by high-average-power femtosecond NIR pulses. The strongest MIR noise suppression – up to a factor of 20 – was attained when stabilizing to the red edge of the broadened NIR spectrum. We demonstrated a RIN of the MIR intensity of 0.05% rms over a time period of 10 min (this is equal to a frequency noise bandwidth of 2 mHz to 2 Hz). A minimal RIN value of 6 * 10^{-7} $Hz^{-0.5}$ was obtained at 10 kHz.

MIR spectroscopic techniques, like FTIR or direct absorption spectroscopy, would directly benefit from the proposed noise suppression system, as the interfering noise frequencies are usually located at kHz frequencies and below. Additionally, the error signal for the feedback is derived from the driving NIR beam, so that no liquid-nitrogen-cooled MCT detectors are necessary. This factor, together with the reduced intensity noise and MIR

Optics EXPRESS

detection schemes that rely on frequency-up-conversion [8,16,17], should facilitate the realization of highly sensitive MIR spectroscopy that does not require any MIR detectors.

The stabilization schemes presented here can be easily adapted for other laser-driven light and electron sources which suffer from intensity noise and cannot easily be stabilized due to the lack of active optical elements or adequate detectors.

6. Appendix

6.1. Calculation of the shot noise limit of the stabilization scheme

Quantum or shot noise is a fundamental noise limit imposed by the photon nature of light. The relative shot noise power of a light source at a central wavelength λ and an average power of P can be calculated with

$$s_q = \sqrt{\frac{2hc}{P\lambda}} \tag{2}$$

where h is the Planck constant and c is the speed of light in the vacuum. For a given feedback system, the relative shot noise of the light impinging on the in-loop (with power P_{IL} and central wavelength λ_{IL}) and out-of-loop (with power P_{OOL} and central wavelength λ_{OOL}) photodetectors contribute to the attainable shot noise limit s_{tot} of the stabilization system [13]:

$$s_{tot} = \sqrt{\frac{2hc}{P_{IL}\lambda_{IL}} + \frac{2hc}{P_{OOL}\lambda_{OOL}}} \tag{3}$$

For the system presented here, the error signal was generated with a 0.7-mW NIR beam (at ≈1 μm) and the MIR beam (at ≈10 μm) had an average power of 0.07 mW. This gives a relative shot noise limit for the stabilization system of $3 * 10^{-8}\ Hz^{-0.5}$

6.2. Active intensity noise suppression of the near-infrared pulse train

The stabilization system for the MIR light can also be used to stabilize the intensity noise of the driving NIR light. The levels of RIN for the free-running NIR beam and the red edge of the broadened NIR spectrum are depicted in Fig. 6(a). The degrees of noise suppression attained by the different stabilization concepts are show in Fig. 6(b)-6(d) and values of the integrated noise and the noise reduction at 5 kHz are given in Table 1.

Table 1. NIR noise suppression

Stabilization concept	Noise reduction at 5 kHz	Integrated RIN (from 1Hz to 100 kHz)
Free running	-	0.1
1	30	0.021
2a	29	0.006
2b	1.7	0.04
3a	15	0.007
3b	0.08	1.3

In general, better noise suppression can be achieved for NIR than for MIR (up to a factor 30 instead of 20 and an integrated RIN of 0.006% instead of 0.07%). This is not surprising, as the error signal is derived from the very beam that is subjected to stabilization, and therefore one non-linearity less is involved. However, stabilization concept IIIb, which worked best on the MIR, yields only a small noise suppression of about a factor 2 for the NIR. Indeed, stabilization concept Ib actually worsens the RIN of the broadened NIR by a factor of 11. This effect is due to the broadband nature of the NIR radiation. Concepts Ib and IIIb both use

Optics EXPRESS

the red edge of the broadened spectra to generate the error signal. As discussed above, the intensity noise within the edges of the broadened spectra is nonlinearly linked to input intensity fluctuations, whereas the fluctuations of the fully broadened NIR are approximately proportional to the input fluctuations (if no losses occur, the output power of the fiber equals the input power) and therefore there may be no linear correlation between the intensity fluctuations of the full NIR beam and those of red part of the spectrum. Additionally, the RIN of the red part of the spectrum is augmented due to the fiber broadening (see Fig. 6(a), black vs gray curve). This part of the spectrum is used to generate the error signal in concept Ib. With active feedback, the AOM compensates for those fluctuations; however, as there is no correlation between the red part of the spectrum and the full spectrum, it introduces additional noise in the rest of the spectrum, as it acts on the full NIR beam. Concept IIIb also uses the red part of the spectrum. In contrast to concept Ib, the AOM is placed in front of the nonlinear fiber and therefore actively controls the input power to the fiber to stabilize the power in the red part of the broadened output spectrum. This also leads to suppression of intensity fluctuations of the integrated spectrum (see Fig. 6(d), cyan curve).

In summary, it can be concluded that the choice of a stabilization concept depends on the desired application, as they will differ in their performance. If the goal is to stabilize the NIR output energy of a nonlinear fiber, the suppression works best if the full optical spectrum of the broadened NIR beam is used for generation of the error signal. However, this does not necessarily stabilize the intensity fluctuations at the edges of the optical spectrum and, as shown in the main text (see Fig 4(a)), it might not improve the stability of a DFG output.

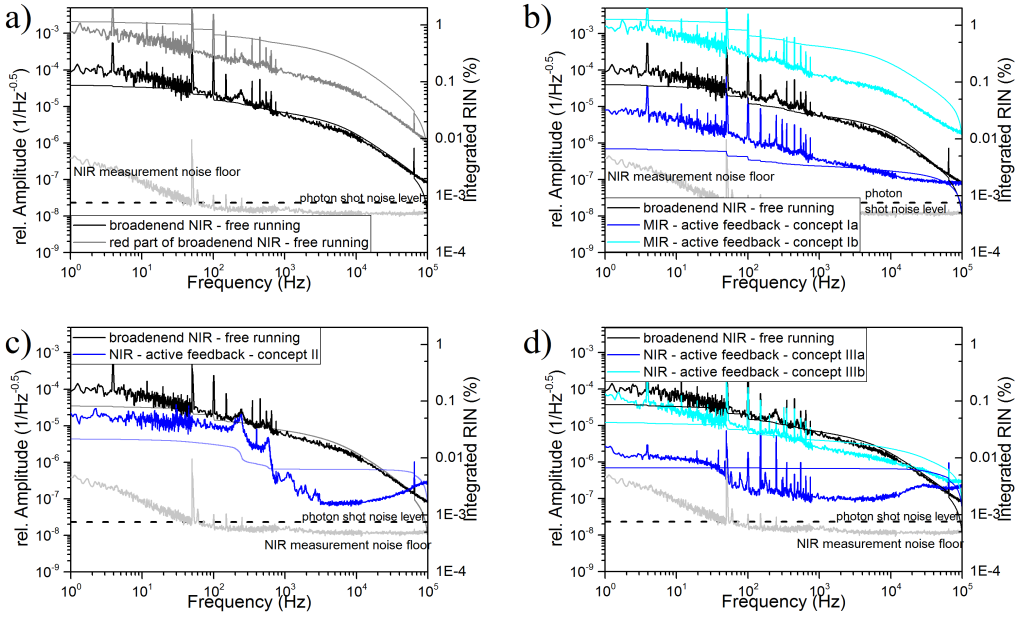

Fig. 6. a) Relative intensity noise and integrated noise (integration starts at 100 kHz) of the free running system for the oscillator (black) and the broadened NIR (gray). b)-d) NIR noise suppression for the different stabilization concepts. Strong NIR noise suppression is only obtained when stabilizing to the full (spectrally integrated) NIR signal.

If the goal is to stabilize the intensity fluctuations within different parts of the optical spectrum and therefore stabilize the spectral broadening itself, the suppression works best if one uses the edge of the broadened NIR to generate the error signal. This approach does not markedly suppress the RIN of the full NIR beam (see Fig. 6(d), cyan curve), but it does lead to a major improvement in the stability of the MIR generated via intra-pulse DFG (see Fig 4(a)).

Optics EXPRESS

6.3. Relative intensity noise of the free-running broadened NIR and MIR pulse train for frequencies up to 1 MHz

To measure the RIN spectrum of the free-running NIR or MIR beam up to 1 MHz, we used the same photodiodes as before. The noise spectrum was obtained via FFT of the photodiode signal measured with a MHz-Lock-In amplifier (Zürich Instruments, UHFLI) and is displayed in Fig. 7. The RIN of the NIR light approaches the shot noise limit around 200 kHz before the measurement is limited by the detector noise floor.

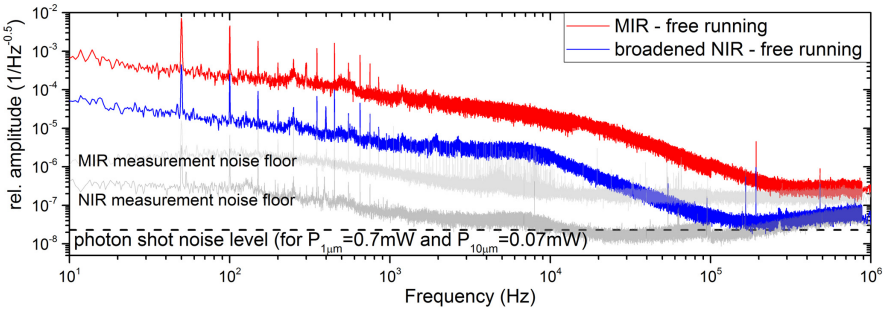

Fig. 7. Relative intensity noise spectrum free-running broadened NIR and MIR pulse train.

Funding

Munich Centre for Advanced Photonics (www.munich-photonics.de), a DFG-funded Cluster of Excellence.